Acta Polytechnica **62**(3):400–408, 2022
https://doi.org/10.14311/AP.2022.62.0400

Published by the Czech Technical University in Prague

EXPERIMENTAL VERIFICATION OF THE IMPACT OF THE AIR STAGING ON THE NO_X PRODUCTION AND ON THE TEMPERATURE PROFILE IN A BFB

Matěj Vodička*, Kristýna Michaliková, Jan Hrdlička, Pavel Skopec, Jitka Jeníková

Czech Technical University in Prague, Faculty of Mechanical Engineering, Department of Energy Engineering, Technická 4, 166 07 Prague, Czech Republic

* corresponding author: matej.vodicka@fs.cvut.cz

Abstract.

The results of an experimental research on air staging in a bubbling fluidized bed (BFB) combustor are presented within this paper. Air staging is known as an effective primary measure to reduce NO_X formation. However, in the case of a number of industrial BFB units, it does not have to be sufficient to meet the emission standards. Then selective non-catalytic reduction (SNCR) can be a cost-effective option for further reduction of the already formed NO_X. The required temperature range at the place of the reducing agent injection for an effective application of the SNCR without excessive ammonia slip is above the temperatures normally attained in BFBs. The aim of this paper is to evaluate the impact of staged air injection on the formation of NO_X in BFB combustors and to examine the possibility of increasing the freeboard temperature. Several experiments with various secondary/primary air ratios were performed with a constant oxygen concentration in the flue gas. The experiments were carried out using wooden biomass and lignite as fuel in a 30 kW_{th} laboratory scale BFB combustor. Furthermore, the results were verified using a 500 kW_{th} pilot scale BFB unit. The results confirmed that the air staging can effectively move the dominant combustion zone from the dense bed to the freeboard section, and thus the temperatures for an effective application of the SNCR can be obtained.

Keywords: Air staging, bubbling fluidized bed, NO_X, SNCR.

1. Introduction

Nitrogen oxides (NO_X), particularly NO and NO_2, are gaseous pollutants that can cause significant environmental issues. One of the main contributors to overall NO_X emissions is the combustion of solid fuels.

There are three mechanisms of NO_X formation in the combustion process: the thermal and prompt NO_X formation mechanism, where the source of NO_X is atmospheric nitrogen, and the oxidation of fuel-bound nitrogen. Since the breaking of tight N_2-bond is strongly temperature dependent, the thermal NO_X formation mechanism (described by Zeldovich et al. [1]) is usually considered important at temperatures higher than 1500 °C [2]. Then, the prompt formation of NO_X (described by Fenimore [3]) can be observed in fuel-rich zones in pre-mixed hydrocarbon flames. The prompt NO_X formation is also strongly temperature dependent and is relevant from above 1400 °C. These conditions are not typical for combustion in bubbling fluidized beds (BFBs) and therefore prompt and thermal NO_X are of minor importance, and fuel-bound nitrogen is considered to be the main contributor to NO_X formation there [4–6]. Fuel-bound nitrogen is an important source of NO_X in the combustion of fossil fuels and biomass. It is particularly important for coal combustion, which typically contains $0.5 - 2.0$ % wt. of nitrogen, and for the combustion of non-wooden biomass, where its content can reach up to 5 % wt. The degree of conversion of fuel-N to NO_X is almost independent of the type of nitrogen compound, but is significantly dependent on the local combustion environment [7]. In the furnace, fuel is thermally decomposed and volatile and char compounds are produced. Fuel-bound nitrogen is distributed between char and volatiles, depending on the fuel structure and devolatilisation conditions, such as temperature, heating rate, oxygen concentration, or residence time. In case of lower temperatures or shorter residence times, nitrogen preferably remains in the char, while at higher temperatures, it is part of the volatiles [8]. The mechanisms of volatile-N and char-N conversion were described by Winter et al. [9], who studied the combustion of a single particle of bituminous coal, subbituminous coal and beech wood in an electrically heated, laboratory-scale, fluidized bed combustor.

The NO_X reduction can be generally realized using different methods; either by modifying the combustion process itself to supress the NO_X formation (so-called primary measures) or applied after the combustion process to decrease the already formed NO_X (so-called secondary measures). Skopec et al. [6] observed using a 500 kW_{th} BFB combustor that the NO_X formation depends mainly on the excess of oxygen in the combustion zone and slightly also on the fluidized bed temperature. This was also confirmed by Svoboda

and Pohořelý [10], who studied the formation of NO_X and N_2O in a laboratory scale pressurized BFB. They observed that NO_X formation was strongly promoted by an increase in air stoichiometry (while N_2O formation was depressed) at atmopheric pressure. They also observed that an increase in the temperature of the fludized bed slightly promotes the formation of NO_X and decreases the formation of N_2O under slightly elevated pressure (0.25 MPa). Therefore, the primary measures reduce the temperature and oxygen concentration in the furnace and subsequently allow the oxidation of the remaining combustibles above the furnace. As primary measures, staged injection of air or fuel and flue gas recirculation could be used. Fuel staging requires secondary gas phase fuel and it is not a practically applied method for BFBs.

In the case of staged air injection, the oxidizer is separated into two or even more streams. The first stream is introduced into the BFB as the primary air (possibly mixed with the FGR). The second stream (and possibly the consequent streams) is introduced into the freeboard section above the fluidized bed. In the primary combustion zone, there are fuel-rich conditions (stoichiometric or even sub-stoichiometric oxygen/fuel ratio) that cause a smaller conversion of the NO_X precursor to NO_X and favor the formation of N_2. Furthermore, the already formed NO can be further reduced through a) reburning reactions with the released fuel N (mainly HCN and NH_3), or b) through reactions with carbon compounds that were not yet completely oxidized, or c) on the char surface through catalytic reactions [11, 12]. Gaseous products of incomplete combustion (CO and TOC), which are inevitably formed under such conditions, are subsequently oxidized in the freeboard section, where the secondary oxidizer is introduced. The efficiency of NO_X reduction through staged injection of air is significantly dependent on the residence time in the primary zone with sub-stoichiometric (reduction) conditions [12, 13]. The optimum residence time in the sub-stoichiometric zone may vary according to the fuel structure. For a lignite coal, it is about 1.5 s [13]. If the residence time in the this zone is too short, NO can further form in a significant amount in the secondary oxidation zone [12]. Sirisomboon and Charernporn [14] also observed that the relative reduction efficiency of the staged air injection depends on the overall stoichiometry of the combustion air. With the most extensive air staging, they observed a similar reduction of about 70 ppmv of NO at all air excess ratios (in the range from 20 to 80 %). Since the formation of NO_X is strongly affected by overall air stoichiometry, the reduction efficiency was higher for lower excess of air and lower for higher excess of air.

Secondary measures are mainly selective non-catalytic (SNCR) and selective catalytic reduction (SCR). These flue gas treatments use reducing agents containing NH_2 (ammonia, urea, ammonia water, etc.), which can reduce NO. The reduction follows

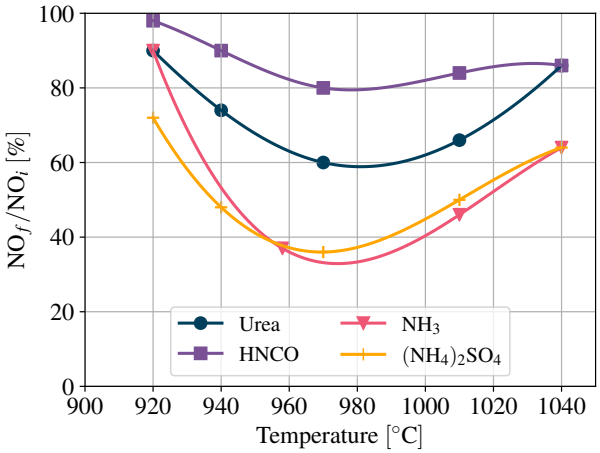

FIGURE 1. Comparison of the dependence of the NO_X reduction efficiency (expressed as a ratio of the final NO_X concentration with SNCR to the initial NO_X concentration without SNCR) using urea, cyanuric acid, ammonia and ammonium sulfate on the flue gas temperature [15].

Equation 1 in the case of using ammonia as a reducing agent

$$2\,NO + 2\,NH_3 + \frac{1}{2}\,O_2 \longrightarrow 2\,N_2 + 3\,H_2O \quad (1)$$

and Equation 2 in the case of using urea.

$$2\,NO + CO(NH_2)_2 + \tfrac{1}{2}\,O_2 \longrightarrow 2\,N_2 + CO_2 + 3\,H_2O \quad (2)$$

The effective operation of SNCR without excessive ammonia slip is determined by an optimal temperature range for the injection of the reducing agent into the combustor. The ideal temperature range depends on the reducing agent used, which can be seen in Figure 1. However, the required temperature range 900 – 1000 °C is normally achieved neither in the bed nor in the freeboard in BFBs.

The catalyst present in the SCR systems usually allows achieving higher reduction efficiency at significantly lower temperatures compared to SNCR technology, but at a high investment cost.

Air staging, which partly moves the combustion zone from the dense bed zone to the freeboard of the BFB, appears to be a suitable measure for increasing the freeboard temperature to the required temperature range. Sirisomboon and Charernporn [14] increased the temperature in the freeboard section of a pilot scale BFB of about 100 °C through air staging and reached up to 1 100 °C using high volatile sunflower shells as fuel.

Although NO_X formation and possible reduction paths in BFBs have been studied by a number of authors using multiple fuels and various scales of devices, the possible application of SNCR in BFBs has not been of significant interest yet.

This paper presents a comprehensive experimental study of the impact of staged air supply on NO_X formation in a BFB and on the temperature profile within

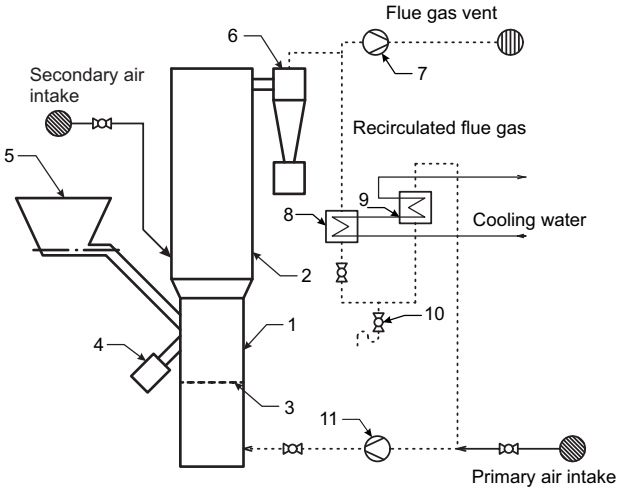

(a) . 30 kW_{th} experimental BFB facility and its equipment.

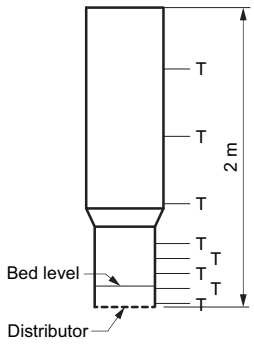

(b) . Indication of temperature measuring points.

Figure 2. Scheme of the 30 kW_{th} experimental BFB facility. 1) fluidized bed region, 2) freeboard section, 3) fluidizing gas distributor, 4) fluidized bed spillway, 5) fuel feeder, 6) cyclone particle separator, 7) flue gas fan, 8) and 9) FGR water coolers, 10) condensate drain, and 11) primary gas fan.

the combustor as a consequence of sub-stoichiometric combustion in the dense bed and subsequent oxidation of the remaining combustibles in the freeboard section in order to be able to define the process conditions for reaching the SNCR optimal temperature range. A number of experiments were performed combusting lignite and wooden pellets in various operating regimes of a 30 kW_{th} BFB experimental facility. Furthermore, to validate the results and their applicability to the industrial scale, the same experiments were performed in a 500 kW_{th} pilot-scale BFB combustor.

2. Experiments

2.1. Experimental setup

The 30 kW_{th} experimental facility has been comprehensively described elsewhere [16] and so it will be described only briefly here. Its scheme is given in Figure 2. The facility is 2 m high, has a rectangular cross-section, and is made of stainless steel insulated from the outside using the 50 mm thick Insulfrax board in the fluidized bed section and using mineral wool

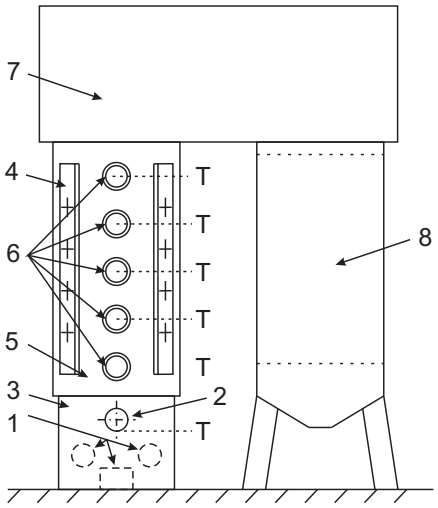

Figure 3. Scheme of the 500 kW_{th} pilot-scale BFB facility. 1) primary gas inlets, 2) fuel feeder, 3) fluidized bed region, 4) secondary air distributors, 5) freeboard section, 6) inspection windows, 7) crossover pass, and 8) heat exchanger. The 'T' signs indicates the temperature measurement points.

in the freeboard section. There are no internal heat exchangers in the facility.

Volumetric flows of primary and secondary air were measured using two rotameters. The temperature profile along the height of the facility was measured using five thermocouples in the dense bed region and three thermocouples in the freeboard region. Directly in the fluidized bed, the temperature was measured with two thermocouples. However, the value of only one placed 166 mm above the fluidizing gas distributor was taken as representative. Primary air with real flue gas recirculation were used to provide sufficient fluidization, and secondary air was introduced at the beginning of the freeboard section. The flue gas was continuously sampled and the volumetric fractions of CO_2, CO, SO_2 and NO_X were measured using a NDIR sensors, while the volumetric fraction of O_2 was measured using a paramagnetic sensor.

The scheme of the 500 kW_{th} pilot scale BFB boiler is given in Figure 3. This boiler consists of three main sections: the combustion chamber with freeboard, the crossover pass, and the heat exchanger. The fluidization gas, formed by primary air and recirculated flue gas, enters the bed trough distributor consisting of 36 nozzles placed in 6 rows. The combustion chamber and the freeboard section have a cylindrical cross section and are insulated with a fireclay lining with a water-cooled surface. In the freeboard area, the facility is equipped with 6 thermocouples along the height. Secondary air is supplied to the freeboard section by 4 distributors placed evenly on a perimeter, and each distributor can provide the secondary air inlet at 4 different heights. For the experiments, secondary air inlets at a height of 550 mm above the fluidized bed were used. From the freeboard section, the flue gas continues to the empty crossover pass

	as received				dry ash free					
	LHV [MJ · kg^{-1}]	water [wt. %]	ash [wt. %]	comb.* [wt. %]	C [wt. %]	H [wt. %]	N [wt. %]	S [wt. %]	O* [wt. %]	volatiles [wt. %]
lignite	17.6	21.1	9.9	69.0	72.3	6.3	1.1	1.3	19.0	47.0
wood	16.4	7.8	1.5	90.7	51.0	6.9	0.3	0.003	41.797	84.6

* Calculated as balance to 100 %.

TABLE 1. Proximate and ultimate analysis of the fuels used within the experiments.

		Liginite ash	LWA 0−2
ρ_s	kg · m^{-3}	2 195	1088
ρ_b	kg · m^{-3}	795	570
d_{mean}	mm	0.37	1.07
d_{mode}	mm	0.23	1.02
d_{10}	mm	0.15	0.54
d_{50}	mm	0.74	1.05
d_{90}	mm	1.77	1.59

TABLE 2. Results of the particle size distribution analysis of the fluidized bed materials.

with water-cooled surface and then enters the heat exchanger. The flue gas was continuously sampled and the volumetric fractions of CO_2, CO, SO_2 and NO_X were measured using NDIR sensors, while the volumetric fraction of O_2 was measured using a paramagnetic sensor.

2.2. MATERIALS

The experiments were carried out using Czech lignite Bílina HP1 135 and pellets from spruce wood as fuel. The proximate and ultimate analyses of lignite and wooden pellets are given in Table 1. Lignite has a significantly higher nitrogen content compared to spruce wood, so the NO_X yields should also be higher in case of combustion of lignite. Spruce wood combustibles contain about 100 % more volatiles compared to lignite, which should move the dominant combustion zone slightly higher in the facility in case of wood combustion. For experiments carried out using the 30 kW_{th} facility, the lignite was sieved to a particle size of up to 7 mm. The lignite ash was used as a bed material in the case of lignite combustion. Biomass combustion experiments were carried out using spruce wood pellets (according to the ENplus A1 standard) and using a lightweight ceramic aggregate (LWA) as an external bed material. The physical properties of the bed materials are given in Table 2. The arithmetic mean, mode, median, 1st decile (d_{10}), and 9th decile (d_{90}) particle size were evaluated. The density and bulk density were analyzed along with the particle size. The lignite ash can be classified as Geldart B particles which are well fluidizable and form vigorous bubbles. The used LWA population referred as '0−2' is on the boundary between B and D particle types in the Geldart classification, where the class D particles are difficult to fluidize in deep beds, they spout, form exploding bubbles or channels [17].

From the analysis of the particle size distribution (PSD), the minimum fluidization velocity, the minimum complete fluidization velocity (defined as u_{mf} calculated for the particle size d_{90}, and the terminal particle velocity were evaluated for two different conditions of the fluidization gas. The numerical approach was taken from [18]. First, the gas properties corresponded to air at 20 °C ($\rho_g = 1.20\,kg \cdot m^{-3}$, $\eta = 1.8 \cdot 10^{-5}$ Pa·s) and secondly to air at 850 °C ($\rho_g = 0.29\,kg \cdot m^{-3}$, $\eta = 3.8 \cdot 10^{-5}$ Pa·s). The fluidizing gas temperature of 850 °C was chosen, because when the fluidizing gas passes through the bed of hot material, it is heated to the bed temperature within a few millimeters above the fluidizing gas distributor [19]. The minimum fluidization velocities of both bed materials were also experimentally verified by measuring the correlation of bed pressure drop and superficial fluidizing gas velocity u_0. This method can be found in [18]. This test was carried out using air at 20 °C as fluidization gas. The calculated minimum fluidization velocities, the complete fluidization velocities, and the terminal velocities, as well as the experimentally determined minimum fluidization velocities, are given in Table 3.

2.3. METHODS

To evaluate the impact of staged air supply on NO_X emissions and on the temperature profile within the BFB combustor in consequence of the substoichiometric combustion in the dense bed and subsequent oxidation of the remaining combustibles in the freeboard, two series of experiments were performed using the 30 kW_{th} BFB experimental facility and using lignite and biomass as fuels. Furthermore, a series of experiments was done using the 500 kW_{th} pilot scale facility and only using lignite as fuel. To highlight this impact and reduce the side effects of fluidized bed temperature, the experiments were carried out with a constant bed temperature of 880 °C and the oxygen level in the dry flue gas maintained at 8 % for wooden pellets and at 6 % for lignite for both facilities. The bed temperature was controlled through the change of volumetric flow or of the composition of the fluidizing gas, which consisted of primary air and recirculated flue gas.

Conditions			Lignite ash	LWA 0−2
calculation (experimental) results				
air at 20 °C	u_{mf}	$\mathrm{m \cdot s^{-1}}$	0.37 (0.42)	0.40 (0.38)
	u_{mf-90}	$\mathrm{m \cdot s^{-1}}$	1.72	0.65
	u_t	$\mathrm{m \cdot s^{-1}}$	2.02	3.09
	u_{t-90}	$\mathrm{m \cdot s^{-1}}$	5.47	4.06
air at 850 °C	u_{mf}	$\mathrm{m \cdot s^{-1}}$	0.21	0.27
	u_{mf-90}	$\mathrm{m \cdot s^{-1}}$	2.59	0.62
	u_t	$\mathrm{m \cdot s^{-1}}$	2.36	4.95
	u_{t-90}	$\mathrm{m \cdot s^{-1}}$	10.23	7.24

Table 3. Minimum fluidization velocities u_{mf}, terminal velocities u_t (calculated for d_{mean}), minimum velocities of complete fluidization u_{mf-90}, and complete terminal velocities u_{t-90} (calculated for d_{90}) of the selected fluidized bed materials. The experimental values are in brackets.

The degree of the combustion air staging can be described using Equation 3.

$$\psi = \frac{V_{air,\,sec}}{V_{air,\,prim}}, \tag{3}$$

where $V_{air,\,sec}$ is the volumetric flow of secondary air and $V_{air,\,prim}$ is the volumetric flow of primary air.

In the experiments performed using 30 $\mathrm{kW_{th}}$ BFB facility, one case without air staging was measured as a reference for both fuels and then the following four cases with an increasing secondary/primary air ratio ψ to 2.75 were measured. The minimum amounts of primary and secondary air were limited by the flowmeters used for the volumetric flows measurement and were set to 10 $\mathrm{m^3_N/h}$. The step for increment of the secondary air flow was 6 $\mathrm{m^3_N/h}$. However, to keep the overall oxygen level constant and maintain the bed temperature and sufficient fluidization, it was not possible to exactly keep the required secondary/primary air ratio constant throughout. A reference case without air staging and three cases with an increasing secondary/primary air ratio ψ up to 1.6 were performed using the 500 $\mathrm{kW_{th}}$ pilot-scale facility.

3. Results and Discussion

The results of biomass and coal combustion in the 30 $\mathrm{kW_{th}}$ facility (given in Figures 4 and 5 and Tables 4 and 5) show that the air staging positively affected $\mathrm{NO_X}$ concentration in the flue gas and the $\mathrm{NO_X}$ formation was suppressed with a higher secondary/primary air ratio. On the other hand, the CO level increased significantly, as can be seen in Figures 4 and 5. This could be caused by the decrease in excess oxygen to a sub-stoichiometric atmosphere in the fluidized bed region ($\lambda_{prim} < 1$) connected with incomplete combustion and increased CO production, which is then not oxidized effectively in the freeboard region, possibly due to lower temperatures there. Therefore, the application of air staging from this point of view is limited by acceptable CO emissions. Unfortunately, the flue gas temperature significantly decreased as

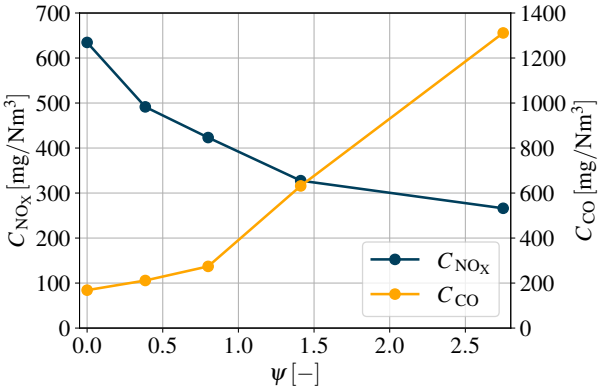

Figure 4. The dependence of the $\mathrm{NO_X}$ and CO volumetric concentration in dry flue gas on the ratio of the secondary to primary air volumetric flows ψ in the case of a lignite combustion in the 30 $\mathrm{kW_{th}}$ BFB facility. The gaseous pollutants concentrations related to 6 % vol. of $\mathrm{O_2}$ in dry flue gas.

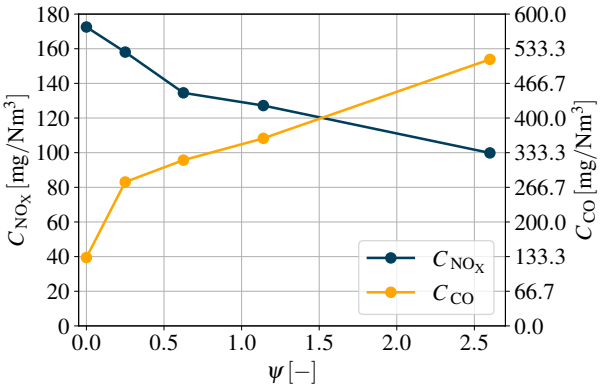

Figure 5. The dependence of the $\mathrm{NO_X}$ and CO volumetric concentration in dry flue gas on the ratio of the secondary to primary air volumetric flows ψ in the case of a biomass combustion in the 30 $\mathrm{kW_{th}}$ BFB facility. The gaseous pollutants concentrations related to 6 % vol. of $\mathrm{O_2}$ in dry flue gas.

Parameter	Unit	'Case 1'	'Case 2'	'Case 3'	'Case 4'	'Case 5'
ψ	[–]	0.0	0.35	0.62	1.23	2.45
λ_{prim}	[–]	1.4	1.04	0.8	0.68	0.48
ϕ_{O_2}	[% vol.]	5.9 ± 0.03	5.93 ± 0.03	5.96 ± 0.03	6.09 ± 0.03	6.13 ± 0.01
t_{BFB}	[°C]	881 ± 0.6	889 ± 0.3	886 ± 0.3	890 ± 0.4	887 ± 0.3
C_{NO_X}	$[mg \cdot m_N^3]$	635 ± 1	491 ± 2	423 ± 1	328 ± 1	266 ± 0
C_{CO}	$[mg \cdot m_N^3]$	277 ± 7	347 ± 4	451 ± 1	1038 ± 5	2155 ± 8
u_0	$[m \cdot s^{-1}]$	1.73	1.73	1.86	1.71	1.71
N – NO	[% mole]	21.61	16.73	14.41	11.16	9.06
m_{fuel}	$[kg \cdot h^{-1}]$	5.8	5.8	5.8	5.8	5.8

TABLE 4. Experimental results of the staged supply of air on the NO_X formation in the case of lignite combustion in the 30 kW_{th} BFB facility. Gaseous pollutant concentrations are related to 6,% vol. of O_2 in dry flue gas.

Parameter	Unit	'Case 1'	'Case 2'	'Case 3'	'Case 4'	'Case 5'
ψ	[–]	0.0	0.25	0.6	1.09	2.29
λ_{prim}	[–]	1.64	1.29	1.03	0.81	0.48
ϕ_{O_2}	[% vol.]	8.21 ± 0.05	8.24 ± 0.04	7.91 ± 0.03	7.93 ± 0.04	7.44 ± 0.03
t_{BFB}	[°C]	888 ± 0.7	894 ± 0.5	888 ± 0.3	890 ± 0.7	897 ± 0.9
C_{NO_X}	$[mg \cdot m_N^3]$	173 ± 0	158 ± 0	135 ± 0	127 ± 0	100 ± 0
C_{CO}	$[mg \cdot m_N^3]$	217 ± 3	455 ± 5	524 ± 5	593 ± 6	843 ± 6
u_0	$[m \cdot s^{-1}]$	2.46	2.35	2.41	2.31	2.31
N – NO	[% mole]	12.01	11.0	9.36	8.85	6.95
m_{fuel}	$[kg \cdot h^{-1}]$	6.9	6.9	6.9	6.9	6.9

TABLE 5. Experimental results of the staged supply of air on the NO_X formation in the case of wood combustion in the 30 kW_{th} BFB facility. Gaseous pollutant concentrations are related to 6 % vol. of O_2 in dry flue gas.

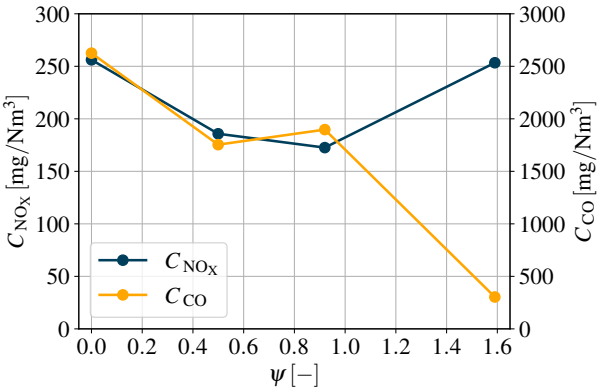

FIGURE 6. The dependence of the NO_X and CO volumetric concentration in dry flue gas on the ratio of the secondary to primary air volumetric flows ψ in the case of a lignite combustion in the 500 kW_{th} BFB facility. The gaseous pollutants concentrations related to 6 % vol. of O_2 in dry flue gas.

the gas passed through the facility due to poor insulation of the freeboard section of the 30 kW_{th} BFB facility. If the temperature is too low at the point of secondary air injection, the oxidation of the unburned combustibles is very slow, which reduces the desired effect of air staging.

Since both the fluidized bed and the freeboard section are well insulated by the fireclay lining in the 500 kW_{th} facility, the freeboard temperatures are significantly higher compared to the 30 kW_{th} facility. Therefore, secondary air properly oxidizes CO and other incomplete combustion products and the concentration of CO does not increase (moreover, it decreases) with an increasing secondary/primary air ratio ψ, as can be seen in Figure 6 and Table 6, where the results of lignite combustion in the 500 kW_{th} BFB facility are given. Based on the rise in the NO_X concentration in flue gas related to the increase in the secondary/primary air ratio ψ from 0.92 to 1.59 in Figure 6, it can be estimated that the NO_X reduction through the air staging has an optimum at the value of the secondary/primary air ratio ψ about 1. The further NO_X reduction observed in the results obtained using the 30 kW_{th} facility can then be explained by the increased CO concentration.

The impact of air staging on the temperature profile in the 30 kW_{th} combustor can be seen in Figures 7 and 8 and on the temperature profile in the 500 kW_{th} combustor in Figure 9.

In the case of the 30 kW_{th} combustor, it was not possible to achieve the temperatures required for SNCR while keeping the bed temperature constant for coal combustion. In the best scenario (for the secondary/primary air ratio ψ 1.4), the temperature rose by 10 °C in a small area directly above the fluidized bed, but this could also be caused by not exactly the same fluidized bed temperature. In general, no significant positive impact was observed from the increase in secondary air supply. In the case of biomass

Parameter	Unit	'Case 1'	'Case 2'	'Case 3'	'Case 4'
ψ	[−]	0.0	0.48	0.91	1.6
λ_{prim}	[−]	1.19	0.7	0.66	0.57
ϕ_{O_2}	[% vol.]	6.06 ± 0.06	5.27 ± 0.04	4.75 ± 0.04	5.73 ± 0.07
t_{BFB}	[°C]	887 ± 0.7	885 ± 0.5	878 ± 0.6	879 ± 0.4
C_{NO_X}	$[mg \cdot m_N^3]$	256 ± 2	186 ± 1	173 ± 1	253 ± 1
C_{CO}	$[mg \cdot m_N^3]$	4314 ± 209	2882 ± 206	3118 ± 236	499 ± 81
u_0	$[m \cdot s^{-1}]$	1.71	1.29	1.02	1.26
N − NO	[% mole]	8.72	6.32	5.87	8.63
m_{fuel}	$[kg \cdot h^{-1}]$	50.0	55.0	46.0	62.0

Table 6. Experimental results of the staged supply of air on the NO_X formation in the case of lignite combustion in the 500 kW_{th} BFB facility. Gaseous pollutants concentrations are related to 6 % vol. of O_2 in dry flue gas.

combustion, enhanced combustion of volatiles above the fluidized bed was observed with an increase in the secondary/primary air ratio, causing a considerable increase in temperature. There, a temperature greater than 900 °C was reached, thus conducive conditions could be provided for the application of SNCR, although the secondary/primary air ratio must be high. However, a significant decrease in freeboard temperatures can be observed for both biomass and coal combustion in Figures 7 and 8, possibly due to insufficient insulation of the freeboard section. The negative impact of staged air supply can be caused by increased volumetric flow, as the higher flow rate is then associated with heat loss. It can be expected that with insulation improvement, air staging would also increase the freeboard temperature for coal combustion, because it did so in the 500 kW_{th} facility, where both the fluidized bed and the freeboard section are insulated using an inner fireclay lining. As can be seen in Figure 9, where the dependence of the temperature height profile on the secondary/primary air ratio ψ is given, staged air injection can move the dominant combustion zone from the furnace to the freeboard section and therefore could increase the freeboard temperature sufficiently for efficient application of SNCR in the BFB boilers even in the case of a lignite combustion. The most significant increase in freeboard temperature was achieved for the secondary/primary air ratio 0.92, where the freeboard temperature was 953 °C for the fluidized bed temperature 880 °C. The further increase in the secondary/primary air ratio did not improve the freeboard temperature but rather cooled it. It can also be seen that the higher volumetric flow of the secondary air and so the higher flue gas velocity in the freeboard section moved the highest temperature measured in the height profile further in the flue gas stream. The increased temperature in the freeboard section invoked by the staged injection of air is also in agreement with the findings of Sirisomboon and Charenporn [14], who carried out the experiments in a well insulated pilot scale BFB.

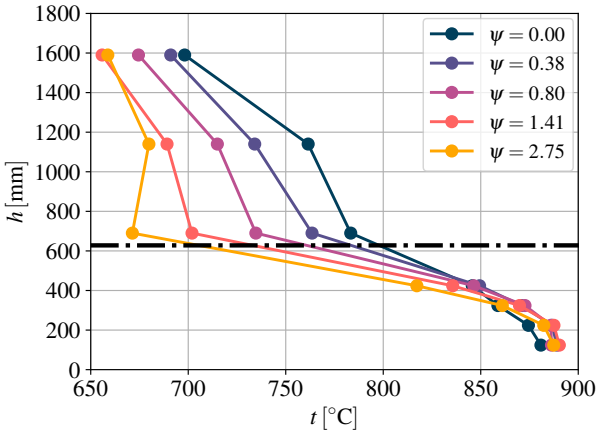

Figure 7. The dependence of the temperature height profile within the 30 kW_{th} BFB facility on the ratio of the secondary to primary air volumetric flows ψ in the case of a lignite combustion. The horizontal dash-and-dot line represents the height where the secondary air is injected.

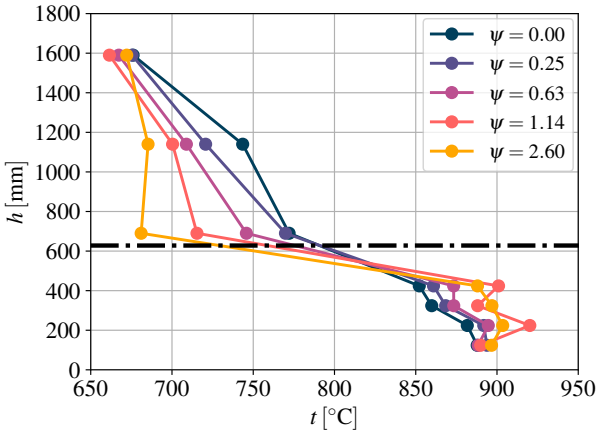

Figure 8. The dependence of the temperature height profile within the 30 kW_{th} BFB facility on the ratio of the secondary to primary air volumetric flows ψ in the case of a biomass combustion. The horizontal dash-and-dot line represents the height where the secondary air is injected.

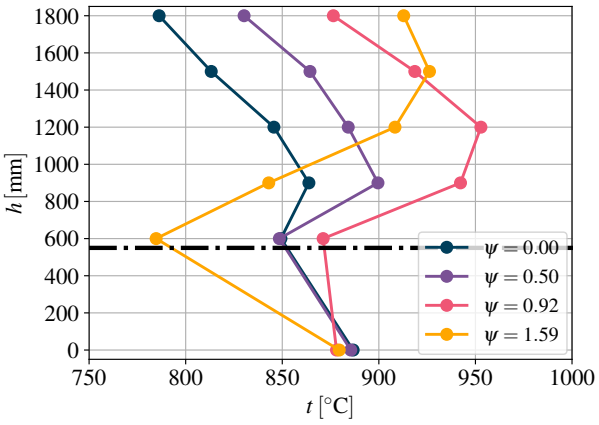

FIGURE 9. The dependence of the temperature height profile within the 500 kW_{th} BFB facility on the ratio of the secondary to primary air volumetric flows ψ in the case of a lignite combustion. The horizontal dash-and-dot line represents the height where the secondary air is injected.

4. CONCLUSION

The aim of the work was to experimentally verify the impact of air staging on NO_X emissions from combustion of coal and wooden biomass in BFB and to study the feasibility of providing sufficient conditions for the application of selective non-catalytic reduction of nitrogen oxides in BFB using two experimental combustors with thermal load 30 and 500 kW_{th}.

The experiments also showed that air staging itself is an effective primary measure for BFB to reduce NO_X formation. In the results from the 30 kW_{th} facility, the suppression of the NO_X directly correlated with an increased secondary/primary air flow ratio. The NO_X emissions reduction efficiency of about 55 % and 40 % was achieved in the case of lignite and biomass combustion, respectively. In the experiments carried out using the 500 kW_{th} facility, the best NO_X emissions reduction efficiency of 33 % was achieved for the secondary/primary air ratio ψ 0.92 and its further increase did not bring further NO_X reduction.

Due to the poor insulation of the freeboard section of the 30 kW_{th} BFB facility, it was not possible to increase the freeboard temperature to a value higher than the fluidized bed temperature for both fuels used. In the case of biomass combustion, the results confirmed that it is possible to reach the suitable temperature range for the SNCR of NO_X by air staging, but the secondary/primary air ratio must be significantly high, resulting in sub-stoichiometric conditions in the dense bed. However, a temperature increase was observed only in the well-insulated fluidized bed region below the secondary air inlets. For coal combustion, no positive impact of staged injection of combustion air was observed in the 30 kW_{th} facility. The experiments carried out with 500 kW_{th} BFB facility showed that if the combustion chamber and the freeboard section are properly insulated, the freeboard temperature increases with the increase of the secondary/primary air ratio. The ideal value of this ratio was approximately 1, for which the freeboard temperature was about 70 °C higher than the fluidized bed temperature. It can be expected that with insulation improvement of the 30 kW_{th} facility, the air staging would have a positive impact on the temperature profile for combustion of both fuels.

Recently, the insulation of the freeboard section of the 30 kW_{th} BFB facility was replaced with Insulfrax boards. Further experiments confirmed that temperature height profiles within the combustor are significantly improved. This study will continue with the characterization of the formation of gaseous pollutants in combustion of alternative biomass fuels in a BFB. In addition, the application of SNCR in the 500 kW_{th} BFB combustor will be studied.

ACKNOWLEDGEMENTS

This work was supported by the Ministry of Education, Youth and Sports under the OP RDE grant number CZ.02.1.01/0.0/0.0/16_019/0000753 “Research centre for low-carbon energy technologies”, which is gratefully acknowledged.

LIST OF SYMBOLS

BFB bubbling fluidized bed
LHV low heating value
LWA lightweight ceramic aggregate
PSD particle sized distribution
SCR selective catalytic reduction
$SNCR$ selective non-catalytic reduction
C_{CO} concentration of CO in the dry flue gas [mg/m^3_N]
C_{NO_X} concentration of NO_X in the dry flue gas [mg/m^3_N]
d_{10} 1st decile particle size [mm]
d_{90} 9th decile particle size [mm]
d_{50} median diameter [mm]
d_{mean} mean particle size [mm]
d_{mode} mode particle size [mm]
h height [mm]
m_{fuel} fuel load [$kg\,h^{-1}$]
N−NO conversion ratio of fuel nitrogen to NO [% mole]
t temperature [°C]
t_{BFB} temperature in the bubbling fluidized bed [°C]
u_o superficial gas velocity [$m\,s^{-1}$]
u_{mf} minimum fluidization velocity [$m\,s^{-1}$]
u_{mf-90} minimum fluidization velocity for d_{90} [$m\,s^{-1}$]
u_{t-90} terminal particle velocity for d_{90} [$m\,s^{-1}$]
u_t terminal particle velocity [$m\,s^{-1}$]
$V_{air\,prim}$ volumetric flow of primary air [m^3_N/h]
$V_{air\,sec}$ volumetric flow of secondary air [m^3_N/h]
λ_{prim} ratio of the air excess in the primary combustion zone [–]
ϕ_{O_2} volumetric fraction of O_2 in dry flue gas [% vol]
ρ_s density of solid material [$kg\,m^{-3}$]
ρ_b bulk density of solid material [$kg\,m^{-3}$]
ψ ratio of the secondary to primary air volumetric flows [–]

References

[1] Y. B. Zeldovich, P. Y. Sadovnikov, D. A. Frank-Kamenetskii. Oxidation of Nitrogen in Combustion. Tech. rep., Academy of Sciences of USSR, Institute of Chemical Physics, Moscow-Leningrad, 1947. Transl. by M. Shelef.

[2] I. Glassman, R. A. Yetter. *Combustion*. Academic Press, Elsevier, 4th edn., 2008.

[3] C. Fenimore. Formation of nitric oxide in premixed hydrocarbon flames. *Symposium (International) on Combustion* **13**(1):373–380, 1971. https://doi.org/10.1016/S0082-0784(71)80040-1.

[4] J. E. Johnsson. Formation and reduction of nitrogen oxides in fluidized-bed combustion. *Fuel* **73**(9):1398–1415, 1994. https://doi.org/10.1016/0016-2361(94)90055-8.

[5] J. Konttinen, S. Kallio, M. Hupa, F. Winter. NO formation tendency characterization for solid fuels in fluidized beds. *Fuel* **108**:238–246, 2013. https://doi.org/10.1016/j.fuel.2013.02.011.

[6] P. Skopec, J. Hrdlička, J. Opatřil, J. Štefanica. NO_X emissions from bubbling fluidized bed combustion of lignite coal. *Acta Polytechnica* **55**(4):275–281, 2015. https://doi.org/10.14311/AP.2015.55.0275.

[7] J. A. Miller, C. T. Bowman. Mechanism and modeling of nitrogen chemistry in combustion. *Progress in Energy and Combustion Science* **15**(4):287–338, 1989. https://doi.org/10.1016/0360-1285(89)90017-8.

[8] P. Glarborg, A. D. Jensen, J. E. Johnsson. Fuel nitrogen conversion in solid fuel fired systems. *Progress in Energy and Combustion Science* **29**(2):89–113, 2003. https://doi.org/10.1016/S0360-1285(02)00031-X.

[9] F. Winter, C. Wartha, G. Löffler, H. Hofbauer. The NO and N2O formation mechanism during devolatilization and char combustion under fluidized-bed conditions. *Symposium (International) on Combustion* **26**(2):3325–3334, 1996. https://doi.org/10.1016/S0082-0784(96)80180-9.

[10] K. Svoboda, M. Pohořelý. Influence of operating conditions and coal properties on NO_X and N2O emissions in pressurized fluidized bed combustion of subbituminous coals. *Fuel* **83**(7-8):1095–1103, 2004. https://doi.org/10.1016/j.fuel.2003.11.006.

[11] H. Stadler, D. Christ, M. Habermehl, et al. Experimental investigation of NO_X emissions in oxycoal combustion. *Fuel* **90**(4):1604–1611, 2011. https://doi.org/10.1016/j.fuel.2010.11.026.

[12] W. Fan, Y. Li, Q. Guo, et al. Coal-nitrogen release and NO_X evolution in the oxidant-staged combustion of coal. *Energy* **125**:417–426, 2017. https://doi.org/10.1016/j.energy.2017.02.130.

[13] H. Spliethoff, U. Greul, H. Rüdiger, K. R. Hein. Basic effects on NO_X emissions in air staging and reburning at a bench-scale test facility. *Fuel* **75**(5):560–564, 1996. https://doi.org/10.1016/0016-2361(95)00281-2.

[14] K. Sirisomboon, P. Charernporn. Effects of air staging on emission characteristics in a conical fluidized-bed combustor firing with sunflower shells. *Journal of the Energy Institute* **90**(2):316–323, 2017. https://doi.org/10.1016/J.JOEI.2015.12.001.

[15] S. L. Chen, J. A. Cole, M. P. Heap, et al. Advanced NO_X reduction processes using -NH and -CN compounds in conjunction with staged air addition. In *22nd Symposium (International) on Combustion*, pp. 1135–1145. The Combustion Institute, Pittsburgh, 1988.

[16] J. Hrdlička, P. Skopec, J. Opatřil, T. Dlouhý. Oxyfuel combustion in a bubbling fluidized bed combustor. *Energy Procedia* **86**:116–123, 2016. https://doi.org/10.1016/j.egypro.2016.01.012.

[17] D. Geldart. Types of gas fluidization. *Powder Technology* **7**(5):285–292, 1973. https://doi.org/10.1016/0032-5910(73)80037-3.

[18] D. Kunii, O. Levenspiel. *Fluidization Engineering*. Elsevier, 2nd edn., 1991. https://doi.org/10.1016/C2009-0-24190-0.

[19] I. G. C. Dryden (ed.). *Fluidized-bed combustion*, pp. 58–63. Butterworth-Heinemann, 2nd edn., 1982. https://doi.org/10.1016/B978-0-408-01250-8.50014-3.